Adsorption (2015) 21:153–163
DOI 10.1007/s10450-015-9658-8

Selective adsorption of ethylene over ethane on natural mordenite and on K^+-exchanged mordenite

D. Vargas-Hernández · M. A. Pérez-Cruz · R. Hernández-Huesca

Received: 20 September 2014 / Revised: 12 January 2015 / Accepted: 14 January 2015 / Published online: 24 January 2015

Abstract Pure-component adsorption equilibrium and kinetics of ethylene (C_2H_4) and ethane (C_2H_6) on natural mordenite (ZNT) from Tamaulipas, Mexico, and on cation-exchanged mordenite samples (1.5 K-ZNT and 1.8 K-ZNT) were measured at 0, 20, 60, and 100 °C using a glass high-vacuum volumetric system. The measured data were analyzed using the Dual Langmuir model. All of the samples showed selectivity toward ethylene. The adsorbed amounts of ethane and ethylene on the 1.5 K-ZNT and 1.8 K-ZNT samples were lower than those on ZNT; this result can be due to a decrease in micropore volume because of the presence of the K^+ cations in the cation-exchanged samples. It was established that the adsorptive separation of these gases on ZNT can be effected most efficiently at 100 °C, whereas the use of 1.8 K-ZNT could be recommended at ambient temperature.

Keywords Mordenite · Ethane · Ethylene · Adsorption equilibrium · Adsorption kinetics

1 Introduction

Olefin/paraffin separations are among the most important processes in the chemical and petrochemical industries. The production of plastics, rubber, films, and other chemicals requires the use of high-purity ethylene (>99.9 %). Ethylene is produced by cracking of ethane. This process produces an ethane/ethylene mixture that has to be separated to produce high-purity ethylene. Cryogenic distillation remains the dominant technology for ethane/ethylene separation due to the similarity in their molecular properties, which leads, for example, to a very low relative volatility of ethylene/ethane (1.5) (Ruthven 1989). Unfortunately, cryogenic distillation has high levels of energy consumption and high equipment costs associated with it. In a typical ethylene-producing plant, cracking equipment represents approximately 25 % of the total cost, while the remainder of the cost is due to the compression, heating, dehydration, recovery, and refrigeration equipment (Anson et al. 2008).

Alternative methods have been considered for the replacement of cryogenic distillation by more economical processes. Some of the new separation techniques being explored include extractive distillation, chemical and physical adsorption, and resin-based membrane separation (Fuertes and Menendez 2002; Eldridge 1993). Selective adsorption is based on the specific interaction between the olefin and chemically modified adsorbents. However, adsorbents based on kinetic or steric effects for the separations of a single olefin from its corresponding paraffin could be used (Yang 1986).

Microporous adsorbents, such as activated carbon, activated alumina, silica gel, and zeolites, can be used to adsorb organic gases. Commonly, transition metal ions (copper or silver) are incorporated into these materials when these are used for olefin/paraffin separation, resulting in the preferential adsorption of the olefin (Yang and Kikkinides 1995; Blas et al. 1998a; Basaldella et al. 2006; Grande et al. 2004; Jiang et al. 2006; Grande and Rodrigues 2004; Giannakopoulos and Nikolakis 2004).

This selective adsorption is due to the strong interaction between the unsaturated bond in the olefin and the metal

D. Vargas-Hernández (✉) · M. A. Pérez-Cruz · R. Hernández-Huesca
Facultad de Ciencias Químicas, Benemérita Universidad Autónoma de Puebla, Edif. 105I-103, 18 Sur y Av. San Claudio, Ciudad Universitaria, 72570 Puebla, PUE, Mexico
e-mail: vargas.diana31@gmail.com

ion in the surface, forming a π-complexation. The idea of exploiting π-complexation dates from the studies made on specific interactions of alkenes with solid cuprous halides reported by Gilliland et al. (1939, 1941). Preferential sorption of the alkene via the formation of π-complexes has been shown to result from charge donor–acceptor interactions between the appropriate atomic and molecular orbitals. Charge donation takes place from the π molecular orbitals of the alkene to the empty atomic orbitals of the transition metal, while back-donation of charge occurs from the d-type atomic orbitals of the metal to the empty antibonding orbitals of the alkene. On the other hand, π-complexation is weaker than the usual ligand coordination and the chemically unchanged alkene molecule may be easily desorbed by increasing the temperature or decreasing the pressure in the system. For adsorptive separation, porous solids possessing high specific areas have been used as substrates and novel cation–substrate combinations have been developed and tested. These include Ag salts on anion-exchange resins (Gilliland et al. 1941; Hirai et al. 1985a), Ag-exchanged resins (Hirai et al. 1985b; Wu et al. 1997), monolayer CuCl/γ-Al_2O_3 (Yang and Kikkinides 1995), monolayer CuCl on pillared clays (Cheng and Yang 1995; Choudary et al. 2002), monolayer $AgNO_3/SiO_2$ (Rege et al. 1998), γ-Al_2O_3, SiO_2, and MCM-41 impregnated by incipient wetness with $AgNO_3$ (Padin and Yang 2000), carbon nanotubes (Albesa et al. 2011), faujasite zeolites (Van Miltenburg et al. 2006), commercial zeolites (such as zeolites 4A, 5A, and 13X) (Da Silva and Rodrigues 1999; Grande et al. 2001; Brandani et al. 1995; Berlier et al. 1995; Grande et al. 2006, 2010; Silva and Rodrigues 2001; Da Silva and Rodrigues 2001; Padin et al. 2000), activated carbon (Choi et al. 2003; Costa et al. 1989; Olivier et al. 1996), carbon molecular sieves (Nakahara and Wakai 1987; Grande and Rodrigues 2004; Rege et al. 1998), and Ag(I)- or Cu(I)-doped adsorbents (Rege et al. 1998; Blas et al. 1998b; Park et al. 2004; Iucolano et al. 2008; Basaldella et al. 2005; Aguilar-Armenta and Patiño-Iglesias 2002). On other hand, the molecular sieving mechanism relies on the exclusion of one component based on size criteria (Chudasama et al. 2005; Lee et al. 2001; Tang et al. 2009). Therefore, because of the small difference between the molecular diameters of C_2H_4 and C_2H_6 (4.163 and 4.443 Å, respectively), there is need for the development of new molecular sieve adsorbents for ethane/ethylene separation (Sircar and Myers 2003).

An evolution in pore size control for crystalline molecular sieves began with the discovery of Engelhard Titanosilicate-4 (ETS-4) (Kuznicki 1990). The crystal lattice of ETS-4 systematically contracts upon dehydration at elevated temperatures. These structural changes can be used to control the lattice dimensions and the channel apertures of ETS-4 to "tune" the effective size of the pores. This phenomenon, known as the molecular gate effect, has achieved commercial success in natural gas purification. For example, Sr-ETS-4 (CTS) adsorbents have been applied to difficult size-based separations including N_2/CH_4 (3.64, 3.76 Å, respectively) on an industrial scale. However, the contraction process irreversibly damages the ETS-4 framework, causing defects in the crystal lattice and reducing the pore volume and the capacity of the adsorbent. Therefore, only certain cation-exchanged adsorbents based on ETS-4 are stable under thermal activation and this limits the usage of molecular gate technology (Lin et al. 2008). Anson et al. have determined that ETS-4 and RPZ materials exchanged with Zn or Ca/H are excellent candidates for the commercial adsorptive separation of ethylene and ethane, due to the molecular sieve character of these adsorbents, and that the contact time between the adsorbent and the ethylene/ethane gas mixture determines the separation thereof (Anson et al. 2010). Among many of the commercial adsorbents, 13X and 4A zeolites have been widely studied and have been proven to be effective adsorbents in vacuum swing adsorption (VSA) processes to obtain high-purity products (Grande et al. 2010; Grande and Rodrigues 2005; Sá Gomes et al. 2009). Da Silva and Rodrigues investigated single-component adsorption isotherms and mass-transfer kinetics of propylene and propane on commercial 13X and 4A zeolites at temperatures between 273 and 473 K. It was found that 13X zeolites show higher adsorption capacity and lower mass-transfer resistance than 4A zeolites, while 4A zeolites show at least one order of magnitude higher selectivity for propylene over propane than 13X zeolites (Da Silva and Rodrigues 1999). Padin et al. reported that commercial 4A zeolite partially modified with Li^+ cations (NaLiA zeolite) has a faster uptake rate of propane than commercial 4A zeolite. In the same work, they also reported that an aluminophosphate (AlPO4-14) is capable of separating propane and propylene by a kinetic effect (Padin et al. 2000). Rege et al. also reported that a kinetically controlled olefin/paraffin separation can be accomplished on zeolite 4A and molecular-sieve carbon, as well as on π-complexation adsorbents (Rege et al. 1998). Li et al. showed that the uptake rate of propene and propane in a serie of zeolitic imidazolate frameworks (ZIFs) can be controlled by the linker size. On ZIF-8, the slightly smaller propene shows a diffusion coefficient which is about 125 times higher than that of propane (at 30 °C) (Li et al. 2009). Wang and Nicholson et al. conducted a grand canonical Monte Carlo (GCMC) simulation to predict the adsorption behavior of ethane and ethylene on $Cu_3(BTC)_2$ (Wang et al. 2008). Lamia et al. demonstrated the feasibility of separation of propane/propylene on a commercial $Cu_3(BTC)_2$ adsorbent using both

experimental measurements and molecular simulations (Sá Gomes et al. 2009). Yoon et al. also explored the adsorptive separation of propylene and propane on $Cu_3(BTC)_2$ that was synthesized using a microwave heating method (Yoon et al. 2010). Recently, novel types of adsorbents called metal–organic frameworks (MOFs) have also been examined for olefin/paraffin separation.

The objective of this work was to measure the pure-component adsorption equilibrium isotherms of ethane (C_2H_6) and ethylene (C_2H_4) on natural mordenite (ZNT) from Tamaulipas, Mexico, and on potassium-cation-exchanged mordenite samples (1.5 K-ZNT and 1.8 K-ZNT), at different temperatures and using a conventional high-vacuum volumetric system. In addition to the study of the adsorption equilibria, the corresponding adsorption kinetics was also measured in order to evaluate the influence of the cation exchange of natural mordenite on the adsorption kinetics of these hydrocarbons. On the basis of the results obtained, we assess the possible use of the adsorbents considered here in the separation of ethylene/ethane mixtures.

2 Experimental

Gas adsorption equilibrium isotherms and gas kinetic uptake were measured at different temperatures in a conventional high-vacuum volumetric device, which is totally made of Pyrex glass and equipped with grease-free valves. High vacuum ($<10^{-4}$ Torr) was achieved using a turbo molecular pump (TSH 062, Balzers), and pressures were registered with two types of pressure transducers (Balzers) of different ranges: TPR 017 (10^{-4}–5 Torr) and APR 011 (1–1000 Torr). Before the equilibrium and adsorption kinetics measurements, all the samples (fraction 0.38–0.54 mm) were first activated in situ by keeping them, for 12 h, in an oven at 300 °C and at a residual pressure of less than 10^{-2} Torr. After this sample dehydration, the temperature was decreased to the desired point and the sample was allowed to stabilize at this temperature for at least 1.5 h before the beginning of the measurements. The measurement temperatures (0, 20, and 60 °C) were controlled by a Haake L water ultrathermostat with a precision of ±0.15 °C, and the temperature of 100 °C was controlled by an oven (Lindberg) with a precision of ±0.2 °C. The adsorbed amount (mmol g^{-1}) of the gases was referred to 1 g of dehydrated adsorbent. The weight loss of the adsorbents was previously evaluated by heating the samples up to 300 °C at atmospheric pressure in a conventional oven. The amount of water desorbed was 11.91, 10.97 and 10.76 % on ZNT, 1.5 K-ZNT, and 1.8 K-ZNT, respectively. Both ethylene and ethane were provided by INFRA (CP grade) with a minimum purity of 99.0 % and were used without further purification.

2.1 Adsorption kinetics measurement

The adsorption of ethylene and ethane as functions of time were obtained on the basis of the difference between the initial amount of gas introduced into the cell and the amount of gas remaining in the dead space of the cell at any given time t_i between $t = 0$ and $t = t_{eq}$ (where t_{eq} is the time needed to reach equilibrium). During the kinetic measurements, the decrease of pressure in the system was measured automatically with a custom acquisition data card, which allows simultaneous monitoring and recording of time and pressure. Pressure was recorded five times per second in the period 0–3 min, once per second in the period 3–13 min, and once every 10 s in the period from 13 min to t_{eq}. In all experiments, the initial pressure was 433 Torr.

2.2 Ion exchange

The chemical modification of the ZNT sample was performed as follows: before the cation-exchange treatment, the ZNT sample was washed with distilled water to eliminate soluble impurities and then dried at room temperature. A 1 g amount (fraction 0.30–0.40 mm) of dry adsorbent was placed in a glass ion-exchange column of 1.4 cm diameter and 12 cm length and held at 60 °C. Then, 200 mL of an aqueous solution of KCl (0.5 M) were percolated through the sample. This cation-exchange procedure was carried out at 65 °C for 1.0 to 2.0 h and, after that, the sample was dried at room temperature.

3 Results and discussion

3.1 Characterization of the samples

The chemical compositions of the samples are shown in Table 1 and were obtained using an atomic absorption spectrophotometer (Perkin Elmer AAnalyst 100). The amount of K_2O was 0.49, 1.50 and 1.8 % for the ZNT, 1.5 K-ZNT and 1.8 K-ZNT samples, respectively. These data show that Na^+ and Ca^{2+} were partially replaced by K^+ (Table 1).

Table 1 Chemical composition (oxide %) of the samples

Sample	CaO	K_2O	Na_2O
ZNT	1.75	0.49	1.63
K1.5-ZNT	0.11	1.50	0.41
K1.8-ZNT	0.24	1.80	0.71

3.2 Equilibrium adsorption

(a) *ZNT* Figures 1 and 2 show the equilibrium adsorption isotherms of pure C_2H_6 and C_2H_4 on ZNT at 0, 20, 60, and 100 °C. These figures show that the amount adsorbed increases continuously with pressure, and decreases with increasing temperature. Considering that mordenite (ZNT) adsorbs molecules with a critical diameter (σ) not exceeding 3.9 Å (Breck 1974) and that σ (C_2H_6) = 3.72 Å and σ (C_2H_4) = 3.44 Å, it is obvious that the adsorption of ethane and ethylene on this adsorbent is not limited by the steric factor, i.e., C_2H_6 and C_2H_4 molecules freely penetrate the entrance windows towards the micropores.

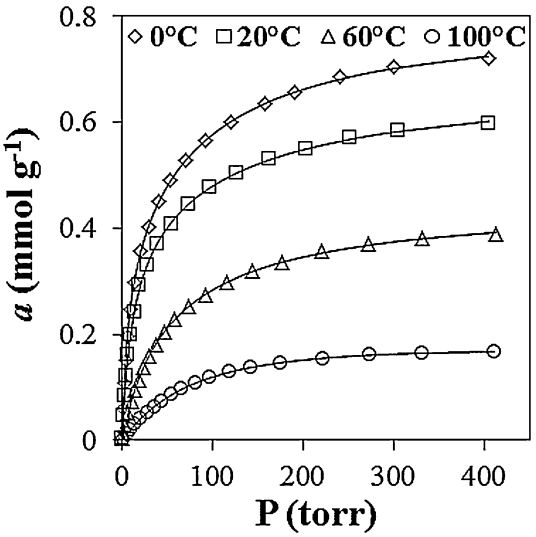

Fig. 1 Adsorption isotherms (*empty symbols*) and Dual Langmuir fit (*solid line*) for C_2H_6 on ZNT at different temperatures

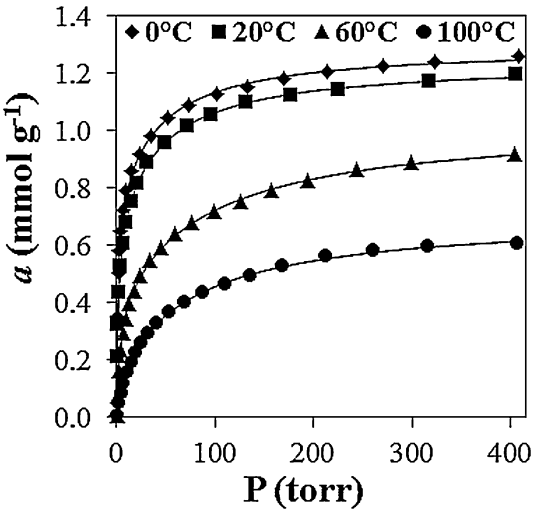

Fig. 2 Adsorption isotherms (*full symbols*) and Dual Langmuir fit (*solid line*) for C_2H_4 on ZNT at different temperatures

All the isotherms in Figs. 1 and 2 are of type I and were fitted using the dual Langmuir (DL) equation,

$$a = a_{m1}\frac{K_1 P}{1 + K_1 P} + a_{m2}\frac{K_2 P}{1 + K_2 P}, \quad (1)$$

with a correlation coefficient $R^2 \geq 0.999$. This equation takes into account the interactions between adsorbed molecules and two energetic adsorption sites (sites 1 and 2). In this equation, a is the amount adsorbed in equilibrium at pressure P, a_{m1} and a_{m2} are the maximum adsorbed amounts, and K_1 and K_2, the adsorption equilibrium constants, for adsorption sites 1 and 2, respectively. The fitting of experimental data with this equation was done using a computational program written in Matlab (Do 1998), and the optimal values obtained for the parameters are given in Table 2.

The total saturation capacity (a_D) (Mathias et al. 1996) is

$$a_D = a_{m1} + a_{m2} \quad (2)$$

As shown in Table 2, the values of the DL constants K_1 and K_2 for C_2H_4 are larger than those for C_2H_6 and this indicates the stronger interaction of C_2H_4 with ZNT because of the contribution of π-bonds to the interaction total energy. As expected, an increase in the temperature led to a decrease in the adsorbed amounts of C_2H_4 and C_2H_6.

To fit the equilibrium isotherm for ethane on ZNT at 100 °C, a negative value of −0.351 mmol g^{-1}, which is physically unacceptable, was obtained for a_{m2}. However, the total saturation capacity a_D, i.e., the maximum

Table 2 Dual-Langmuir Equilibrium Constants for ethane and ethylene on ZNT

	Temperature (°C)			
	0	20	60	100
C_2H_4				
a_{m1} (mmol g^{-1})	0.704	0.660	0.417	0.216
K_1 (torr)	1.392	0.685	0.282	0.095
a_{m2} (mmol g^{-1})	0.592	0.583	0.620	0.492
K_2 (torr)	0.028	0.025	0.011	0.011
C_2H_6				
a_{m1} (mmol g^{-1})	0.332	0.380	0.196	0.499
K_1 (torr)	0.181	0.096	0.034	0.007
a_{m2} (mmol g^{-1})	0.478	0.301	0.257	−0.351
K_2 (torr)	0.012	0.008	0.011	0.004

$-\Delta H_{C_2H_4}$: 21.41 kJ mol^{-1}; $-\Delta H_{C_2H_6}$: 23.33 kJ mol^{-1}

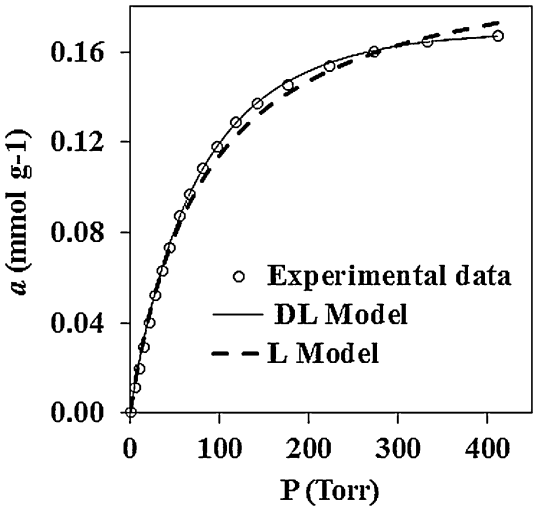

Fig. 3 Adsorption isotherms (*empty symbols*), Dual Langmuir fit (*solid line*), and Langmuir fit (*dashed line*) for C_2H_6 on ZNT at 100 °C

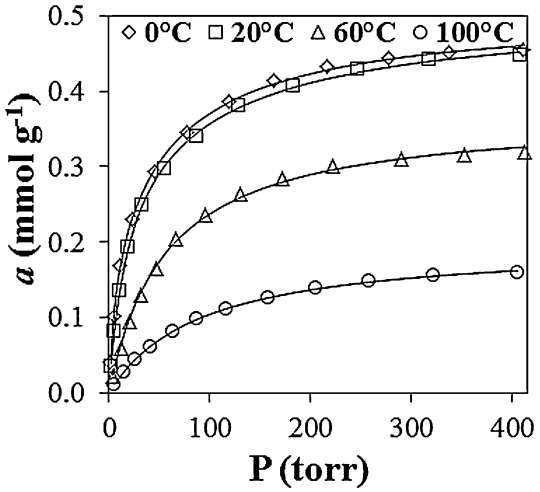

Fig. 4 Adsorption isotherms (*empty symbols*) and Dual Langmuir fit (*solid line*) for C_2H_6 on 1.5 K-ZNT at different temperatures

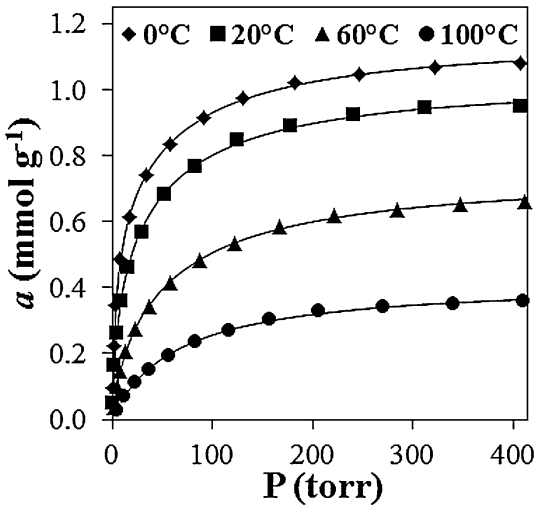

Fig. 5 Adsorption isotherms (*full symbols*) and Dual Langmuir fit (*solid line*) for C_2H_4 on 1.5 K-ZNT at different temperatures

adsorbed amount of C_2H_6 at 100 °C, is positive and equal to 0.148 mmol g^{-1}.

For the purpose of comparison, Fig. 3 shows, together with the Dual Langmuir fit of the equilibrium isotherm for C_2H_6 at 100 °C, another fitting curve found using the Langmuir model (L). Although a good coefficient of determination $R^2 = 0.9937$ for the Langmuir plots (P/*a* vs P) of the C_2H_6 adsorption isotherms was obtained, a good description of the adsorption equilibrium data was observed mainly at low pressures, with deviations at high pressure because one or various assumptions made in this ideal theory are not fulfilled. The values of the Langmuir constant and the maximum adsorbed amount were 0.012 $Torr^{-1}$ and 0.20 mmol g^{-1}, respectively. Therefore, the data in Table 2 show that the dual Langmuir equation was found to fit better the C_2H_6 adsorption isotherms with a correlation coefficient $R^2 \geq 0.999$.

(b) *1.5 K-ZNT* The equilibrium isotherms for both gases on 1.5 K-ZNT at different temperatures are of type *I* and were fitted using the Dual Langmuir model, as in the case of the ZNT sample (Figs. 4 and 5). From these figures, it can be seen that the adsorbed amounts of both hydrocarbons on the 1.5 K-ZNT sample are lower than those on the ZNT sample (Figs. 1 and 2). The values of the DL constants are also lower than those obtained for the ZNT case (Table 3). The lowering of the adsorption capacity and adsorbate–adsorbent interactions for 1.5 K-ZNT as compared with ZNT could be due to the decrease in micropore accessibility and basicity of mordenite with a larger content of K^+ cations (Table 4). The objective of introducing larger cations, such as K^+ (1.33 Å), into the crystal structure of the ZNT sample was to reduce the diffusion rate of C_2H_6 without affecting the diffusion rate of C_2H_4. This, however, is a difficult goal to attain because of the very small difference between the molecular diameters of C_2H_4 and C_2H_6 (3.44 and 3.72 Å, respectively).

(c) *1.8 K-ZNT* Further insight into the interactions between C_2H_4 or C_2H_6 and the cation-exchanged adsorbents may be obtained by examining the adsorption equilibrium isotherms for both hydrocarbons on the 1.8 K-ZNT sample (Figs. 6 and 7). Our results show that there are additional reductions in the adsorbed amounts of C_2H_4 and C_2H_6 which are

Table 3 Dual-Langmuir equilibrium constants for ethane and ethylene on 1.5 K-ZNT

	Temperature (°C)			
	0	20	60	100
C_2H_4				
a_{m1} (mmol g^{-1})	0.580	0.397	0.193	0.006
K_1 (torr)	0.299	0.251	0.110	0.089
a_{m2} (mmol g^{-1})	0.588	0.645	0.563	0.416
K_2 (torr)	0.017	0.019	0.014	0.015
C_2H_6				
a_{m1} (mmol g^{-1})	0.183	0.331	0.194	0.100
K_1 (torr)	0.166	0.054	0.018	0.011
a_{m2} (mmol g^{-1})	0.323	0.179	0.176	0.099
K_2 (torr)	0.016	0.008	0.018	0.011

$-\Delta H_{C_2H_4}$: 10.34 kJ mol^{-1}; $-\Delta H_{C_2H_6}$: 16.68 kJ mol^{-1}

Table 4 Cation properties

Cation	r_i (Å)	e (eV)
K^+	1.33	0.82
Na^+	0.95	0.93
Ca^{2+}	0.99	1.00

r_i ionic radius,
e electronegativity

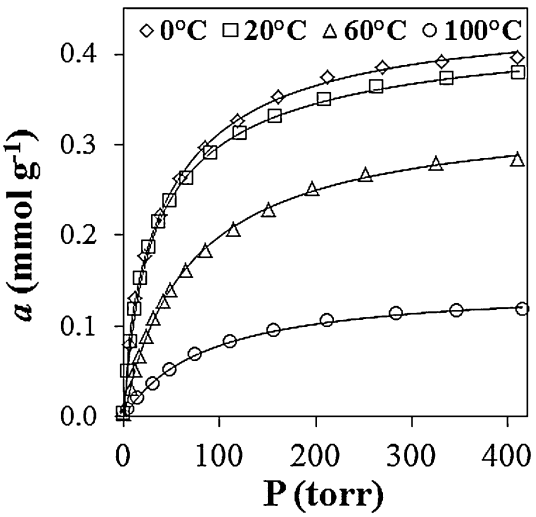

Fig. 6 Adsorption isotherms (*empty symbols*) and Dual Langmuir fit (*solid line*) for C_2H_6 on 1.8 K-ZNT at different temperatures

more important in the lowest temperature isotherms. These results can be due to the further reduction in available pore volume by the replacement of the small cations Na^+ and Ca^{2+} by the larger K^+ cations (Table 4). Obviously, the reduction in pore volume due to the presence of the K^+ cations had more influence on the decrease in the adsorption of ethane, which is the largest molecule.

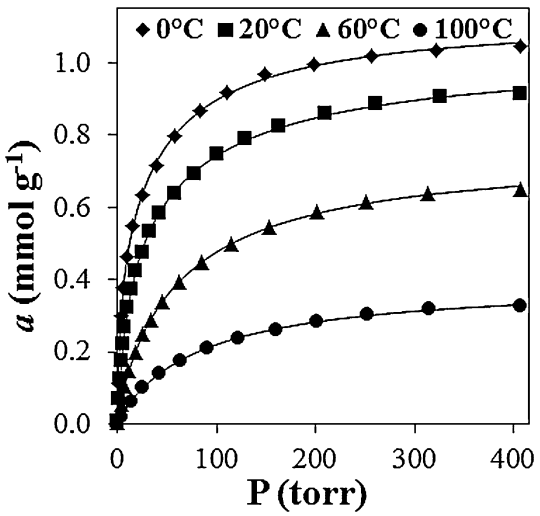

Fig. 7 Adsorption isotherms (*full symbols*) and Dual Langmuir fit (*solid line*) for C_2H_4 on 1.8 K-ZNT at different temperatures

Table 5 Dual-Langmuir equilibrium constants for ethane and ethylene on 1.8 K-ZNT

	Temperature (°C)			
	0	20	60	100
C_2H_4				
a_{m1} (mmol g^{-1})	0.473	0.559	0.137	0.025
K_1 (torr)	0.291	0.088	0.073	0.067
a_{m2} (mmol g^{-1})	0.660	0.472	0.626	0.373
K_2 (torr)	0.020	0.010	0.013	0.011
C_2H_6				
a_{m1} (mmol g^{-1})	0.105	0.310	0.106	0.075
K_1 (torr)	0.194	0.045	0.026	0.012
a_{m2} (mmol g^{-1})	0.343	0.124	0.234	0.071
K_2 (torr)	0.016	0.006	0.011	0.012

$-\Delta H_{C_2H_4}$: 10.06 kJ mol^{-1}; $-\Delta H_{C_2H_6}$: 16.31 kJ mol^{-1}

The experimental isotherms are of type I and were fitted using the Dual Langmuir model with equilibrium constants K_1 and K_2 which have lower values (Table 5) than those for the 1.5 K-ZNT and ZNT cases. However, adsorbate-adsorbent interactions are stronger for C_2H_4, as in the 1.5 K-ZNT and ZNT cases. This could be ascribed to the specific interactions of the ethylene molecules with the cationic adsorption centers via the π orbitals of this olefin. Indeed, the ion-induced dipole interaction, a consequence of the polarization of π-bond electrons by the cations, is the main specific interaction between a cation in the lattice and a C_2H_4 molecule.

These adsorption isotherms were fitted well using the Langmuir model, and for low coverage the experimental points were described by the Henry equation. The

difference in enthalpy between adsorbed and gaseous phases of the sorbate ($-\Delta H$) was evaluated using the van't Hoff equation.

$$\frac{d \ln K_i}{dT} = \frac{\Delta H}{RT_i^2} \quad (3)$$

where K_i is the equilibrium constant in the Langmuir or the Henry equation, R the universal gas constant and T_i the absolute temperature. The values of the equilibrium constants and of the enthalpy of adsorption are given in Tables 2, 3, and 5. Note that the values of the enthalpy of absorption for C_2H_6 are higher than those for C_2H_4 for all the samples. The enthalpy of adsorption ($-\Delta H$) for the adsorption of ethylene were 21.41, 10.34, and 10.06 (kJ mol^{-1}) on ZNT, 1.5 K-ZNT, and 1.8 K-ZNT, whereas for ethane they were 23.33, 16.68, and 16.31 (kJ mol^{-1}) on ZNT, ZNT-K1.5, and ZNT-K1.8, respectively.

3.3 Separation of a binary ethylene/ethane mixture

By comparing the adsorption isotherm data for C_2H_4 and C_2H_6 at different temperatures, as shown in Figs. 1, 2, 3, 4, 5, and 6, it is clear that on all three zeolites the adsorption of C_2H_4 is markedly greater than that of C_2H_6. As mentioned above, it is probable that this result is due to the specific interaction between the π-bonds of the C_2H_4 molecule and the electric field created by the cations present in the structure of the zeolites. The values of the DL equilibrium constants indicate that C_2H_4 is always more strongly adsorbed than C_2H_6 on the three zeolites (Tables 2, 3 and 5). On this basis, it can be assumed that if C_2H_4–C_2H_6 mixtures are put into contact with our three different adsorbents, C_2H_4 would be adsorbed preferentially, leading to an enrichment in C_2H_6 of the gas phase. In Fig. 8, we present the equilibrium compositions of the gas and adsorbed phases for ethane-ethylene mixtures at 100 °C and 100 Torr as predicted by the Ideal Adsorbed Solution Theory (IAST). IAST has been used to predict the adsorption of binary mixtures from the experimental pure gas isotherms (Myers and Prausnitz 1965). It has been reported that IAST can accurately predict gas mixture adsorption in many zeolites (Babarao et al. 2007). Although other theories exist for such predictions, IAST continues to serve as the benchmark for the prediction of adsorption for mixed-gas adsorption from single component isotherms (Murthi and Snurr 2004). In order to perform the integrations required by IAST, the single component isotherms should be fitted by a proper model. There is no restriction on the choice of the model to fit the adsorption isotherm, but data over the pressure range under study should be fitted very precisely.

Adsorption isotherms predicted by IAST for equimolar mixtures of C_2H_6/C_2H_4 in ZNT, 1.5 K-ZNT and 1.8 K-ZNT at 100 °C and 100 Torr are shown in Fig. 8. For all samples, C_2H_4 is preferentially adsorbed over C_2H_6 because of stronger interactions between C_2H_4 and the samples.

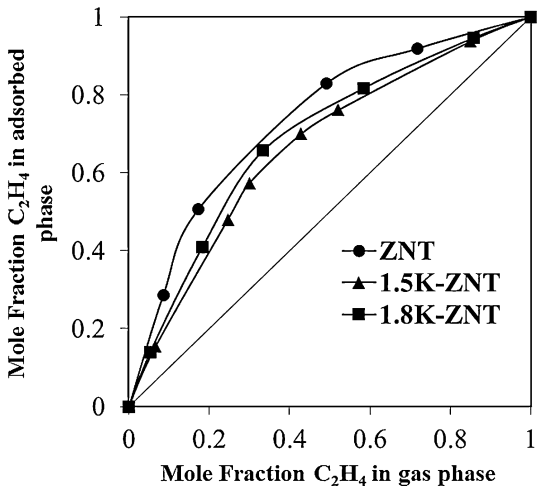

Fig. 8 Gas and adsorbed-phase equilibrium compositions predicted by the Ideal Adsorbed Solution Theory for ethane–ethylene mixtures at 100 °C and 100 Torr

All three equilibrium curves are situated above the diagonal. According to the values of their relative separation efficiency, the three samples can be ordered as follows: 1.5 K-ZNT < 1.8 K-ZNT < ZNT.

3.4 Adsorption kinetics

Adsorbate uptake curves $a = f(t)$ for the two test gases were measured from $t = 0$ up until equilibrium was reached ($t \to \infty$, $a = cons\tan te$).

The kinetic uptakes of C_2H_6 and C_2H_4 on ZNT, at 0, 20, 60, and 100 °C, and for long gas-adsorbent contact times (t ≥ 5000 s), are shown in Figs. 9 and 10, respectively. As can be seen from these figures, the adsorption uptakes for ethane and ethylene increased with increasing temperature.

To better examine the influence of temperature on the adsorption rates of these hydrocarbons, the fractional pore filling a/a_∞, where a and a_∞ are the amounts adsorbed at a given time t and at equilibrium, respectively, was analyzed as a function of time. The results show that the adsorption rate increases with temperature, that is, the activated diffusion of the C_2H_6 and C_2H_4 molecules through the zeolite channels is the rate-controlling process in the adsorption of these gases over the temperature range from 0 to 100 °C. The times $t_{1(0.5)}/(s)$ and $t_{2(0.5)}/(s)$, corresponding to one-half of the fractional uptake ($a/a_\infty = 0.5$) at $T_1 = 0$ °C and $T_2 = 100$ °C, respectively, were 21.6 and 9.8 for C_2H_4 and 443.2, 62.9 for C_2H_6. To estimate the adsorption activation energy E_a of the gases, an equation proposed by Timofeev

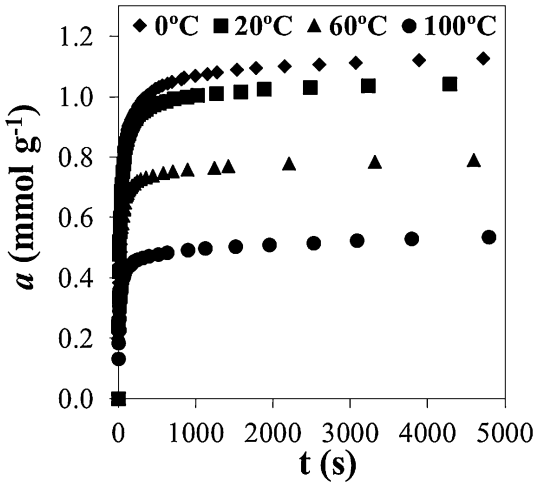

Fig. 9 Uptake rates of C_2H_4 on ZNT at different temperatures

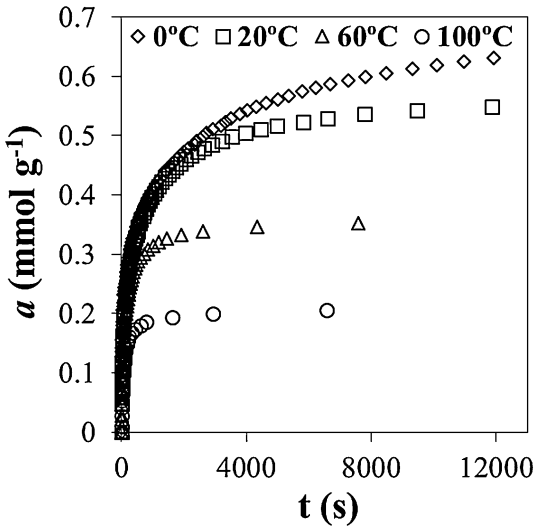

Fig. 10 Uptake rates of C_2H_6 on ZNT at different temperatures

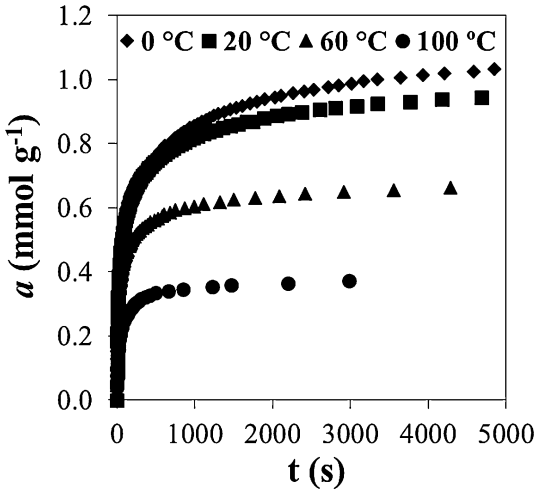

Fig. 11 Uptake rates of C_2H_4 on 1.5 K-ZNT at different temperatures

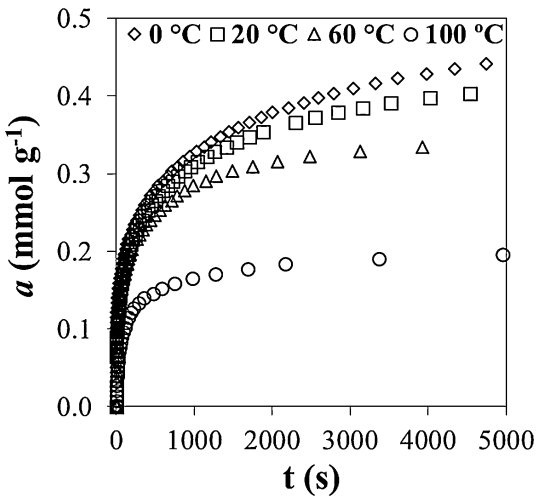

Fig. 12 Uptake rates of C_2H_6 on 1.5 K-ZNT at different temperatures

and Erashko (1961) was used. This equation is the following:

$$E_a = \frac{RT_1T_2}{T_1 - T_2} \ln \frac{t_{2(0.5)}}{t_{1(0.5)}} \quad (4)$$

The activation energies obtained for ethylene and ethane are 6.7 and 16.5 kJ mol^{-1}, respectively. The faster self-diffusion of ethylene can be rationalized by the smaller size of the methylene groups compared to that of the methyl groups. A smaller size means less hindering for crossing the windows of a cavity and hence a smaller apparent activation energy for ethylene is observed (Chmelik et al. 2012). Dewitt et al. have found slightly smaller activation energy values on microporous silica: $E_a(C_2H_4) = (12.5 \pm 2)$ kJ mol^{-1} and $E_a(C_2H_6) = (11.5 \pm 3)$ kJ mol^{-1} (Dewitt et al. 2005); and Romero et al. have found $E_a(C_2H_4) = (13.8 \pm 1)$ kJ mol^{-1} and $E_a(C_2H_6) = (14.6 \pm 0.2)$ kJ mol^{-1} on a 4A (CECA) commercial zeolite sample (Romero-Pérez and Aguilar-Armenta 2010).

The adsorption kinetic behavior at 0, 20, 60, and 100 °C on the 1.5 K-ZNT sample for both gases are presented in Figs. 11 and 12. These results show (Fig. 11) that the ethylene adsorption uptake increases with temperature between 0 and 100 °C.

The adsorption uptake of C_2H_6 increases with temperature, between 0 and 60 °C, and decreases, between 60 and 100 °C (Fig. 12). These results show that the activated adsorptions are predominant for both hydrocarbons over one temperature range (0–60 °C) and that the predominant mechanisms are different over another temperature range (60–100 °C). The fact that the activated adsorption

predominates at higher temperatures for C_2H_4 (up to 100 °C) than those for C_2H_6 (up to 60 °C) could be due to electrostatic contributions (via π-complexation) in the case of the C_2H_4 molecules.

The fractional uptakes $a/a_\infty = f(t)$ for C_2H_4 and C_2H_6 at different temperatures reveal a great difference in the adsorption kinetic behavior of these gases on the ZNT and 1.5 K-ZNT samples. The adsorbed amounts of both C_2H_4 and C_2H_6 on ZNT, in the range from $t = 0$ to $t = t_{eq}$ (equilibrium) at different temperatures, were greater than those on 1.5 K-ZNT. The activation energies on 1.5 K-ZNT were 13.4 and 15 kJ mol^{-1} for ethylene and ethane, respectively. These results show that the diffusion of C_2H_4 rises faster than that of C_2H_6 as the temperature increases. Taking into account that the molecular diameter of ethane is about 3.72 Å, while the ethylene diameter is around 3.44 Å, we believe that these results could be due to the lower micropore participation in the C_2H_6 adsorption process.

The results shown in Figs. 13 and 14 reveal an increase in adsorption uptake when the temperature goes from 0 to 100 °C for C_2H_4 and C_2H_6. These results show that the activated adsorptions predominate.

Unlike for ZNT and 1.5 K-ZNT, the activation energies were 16.20 and 11 kJ mol^{-1} for C_2H_4 and C_2H_6, respectively. This could be due to the reduction of pore volume by the presence of the K^+ cations that greatly influences the adsorption of the ethylene molecule.

To explore the diffusion rate difference between C_2H_4 and C_2H_6, the kinetic adsorption characteristics were measured on ZNT at the same time as the adsorption equilibrium data were collected by a previously described method. As plotted in Figs. 9, 10, 11, 12, 13, and 14, both C_2H_4 and C_2H_6 diffuse faster at higher temperature. To better understand the kinetic behavior, the following micropore diffusion model was used to fit the fractional adsorption uptake curves and to extract the diffusion time constant (D, cm^2 s^{-1}).

During the initial period of adsorption into a constant volume, the fractional uptake can be found from the following equation (Barrer 1971):

$$R = \frac{a_t - a_0}{a_\infty - a_0} = \frac{2S_{ext}}{V}\left(\frac{1+K}{K}\right)\left(\frac{Dt}{\pi}\right)^{1/2} \quad (5)$$

where $K = \left[(a_0)_g - (a_\infty - a_0)\right] / a_\infty$ is the ratio of the adsorbate in the gas phase to that in the adsorbed phase at equilibrium; a_t, a_0 and a_∞ are the amounts of gas adsorbed at times t, $t = 0$, and t = ∞ (equilibrium), respectively (in our experiments $a_0 = 0$); S_{ext} and V are the specific

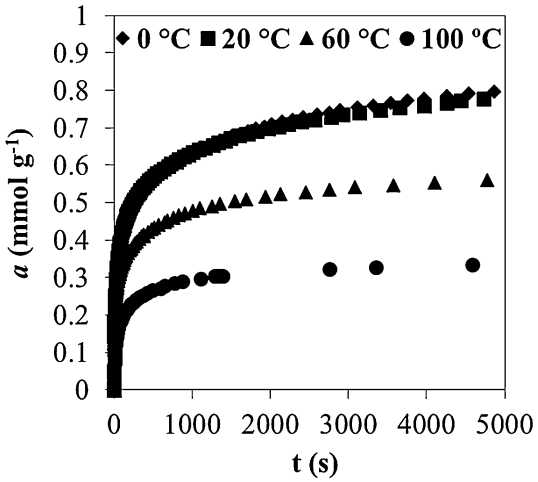

Fig. 13 Uptake rates of C_2H_4 on 1.8 K-ZNT at different temperatures

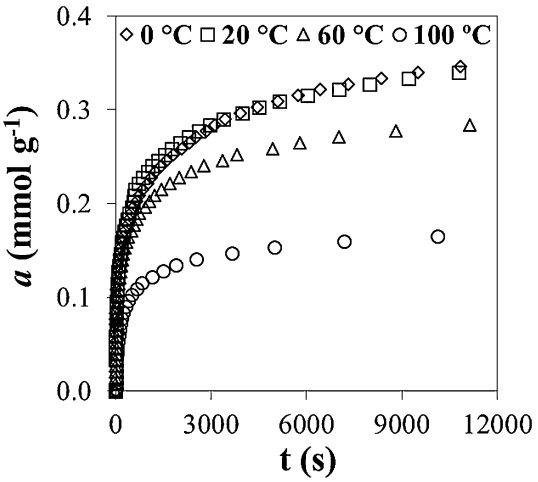

Fig. 14 Uptake rates of C_2H_6 on 1.8 K-ZNT at different temperatures

Table 6 Summary of diffusion time constants and diffusion activation energies of C_2H_4 and C_2H_6 on the three mordenite samples considered in this work

Sample	Temperature (°C)	D × 10^5 (cm^2 s^{-1})		E$_a$ (kJ mol^{-1})	
		Ethylene	Ethane	Ethylene	Ethane
ZNT	0	1.29	0.08	6.7	16.5
	20	2.21	0.15		
	60	3.33	0.38		
	100	3.91	0.70		
1.5 K-ZNT	0	0.38	0.15	13.4	15.0
	20	0.85	0.26		
	60	1.69	0.50		
	100	2.40	0.44		
1.8 K-ZNT	0	0.23	0.11	16.2	11.0
	20	0.42	0.17		
	60	0.92	0.27		
	100	0.74	0.31		

external surface area of the particles ($cm^2\ g^{-1}$) and the volume of the crystals ($cm^3\ g^{-1}$), respectively; $(a_0)_g$ is the amount of gas initially available for adsorption; D is the diffusion coefficient ($cm^2\ s^{-1}$). This model assumes that the mass transfer resistance for gas adsorption is dominated by intracrystalline diffusion, that the adsorbent crystals can be regarded as approximately spherical objects, and that on occasions the kinetic diameter of the gas molecules is comparable with aperture sizes. The values of the diffusion coefficients at different temperatures were found by fitting the experimental data to Eq. (5).

Table 6 summarizes the diffusion time constants and diffusion activation energies of C_2H_4 and C_2H_6 on samples at different temperatures. The diffusion constants of C_2H_4 and C_2H_6 are not the lower order, indicating that a kinetic-based separation is difficult to achieve on samples.

4 Conclusions

Natural mordenite (ZNT) showed a high adsorption capacity for both ethane and ethylene but certain selectivity toward ethylene, because of specific interactions of the ethylene molecules with cationic adsorption centers via the π orbitals of this olefin.

We introduced K^+ cations in the ZNT sample to improve the selectivity toward C_2H_4 but these cations led to sharp decreases in the adsorption capacity for both hydrocarbons, a fact that can be ascribed to a decrease in micropore volume because of the replacement of the Na^+ and Ca^{2+} cations with cations of larger diameter (K^+). Ethylene/ethane separation would occur more efficiently at low temperatures (<20 °C) on 1.5 K-ZNT and 1.8 K-ZNT samples, whereas, at high temperatures, on ZNT.

The adsorption rates of C_2H_4 and C_2H_6 for low t increases with increasing temperature, which means that activated diffusion is the rate-controlling process. The activation energies E_a (kJ mol^{-1}) for the adsorption of ethylene were 6.7, 13.4 and 16.2 on ZNT, 1.5 K-ZNT and 1.8 K-ZNT, whereas for ethane they were 16.5, 15 and 11 on ZNT, ZNT-K1.5 and ZNT-K1.8, respectively.

Acknowledgments The authors thank the Consejo Nacional de Ciencia y Tecnología (CONACyT, Mexico) for financial support via Scholarship No. 219821, and VIEP-BUAP.

References

Aguilar-Armenta, G., Patiño-Iglesias, M.E.: Adsorption equilibria and kinetics of propylene and propane on natural erionite and on erionite exchanged with K+ and Ag+. Langmuir **18**(20), 7456–7461 (2002)

Albesa, A.G., Rafti, M., Rawat, D.S., Vicente, J.L., Migone, A.D.: Ethane/ethylene adsorption on carbon nanotubes: temperature and size effects on separation capacity. Langmuir **28**(3), 1824–1832 (2011)

Anson, A., Lin, C.C.H., Kuznicki, T.M., Kuznicki, S.M.: Separation of ethylene/ethane mixtures by adsorption on small-pored titanosilicate molecular sieves. Chem. Eng. Sci. **65**(2), 807–811 (2010)

Anson, A., Wang, Y., Lin, C.C.H., Kuznicki, T.M., Kuznicki, S.M.: Adsorption of ethane and ethylene on modified ETS-10. Chem. Eng. Sci. **63**(16), 4171–4175 (2008)

Babarao, R., Hu, Z.Q., Jiang, J.W., Chempath, S., Sandler, S.I.: Storage and separation of CO_2 and CH_4 in silicalite, C168 schwarzite, and IRMOF-1: a comparative study from Monte Carlo simulation. Langmuir **23**(2), 659–666 (2007)

Barrer R.M. In: Molecular Sieves Zeolites, Adv. Chem. Ser. 102, American Chemical Society, Washington, DC (1971).

Basaldella, E.I., Tara, J.C., Armenta, G.A., Patiño-Iglesias, M.E., Castellón, E.R.: Propane/propylene separation by selective olefin adsorption on Cu/SBA-15 mesoporous silica. J. Sol-Gel. Sci. Technol. **37**(2), 141–146 (2006)

Basaldella, E.I., Vázquez, P.G., Firpo, N.: Synthesis of Ag/SBA-15 as adsorbent for propane/propylene separation. In *Studies in Surface Science and Catalysis*, edited by N. Ž. a. P. N. J. Čejka: Elsevier, 1081–1088 (2005)

Berlier, K., Olivier, M.G., Jadot, R.: Adsorption of methane, ethane, and ethylene on zeolite. J. Chem. Eng. Data **40**(6), 1206–1208 (1995)

Blas, F.J., Vega, L.F., Gubbins, K.E.: Modeling new adsorbents for ethylene/ethane separations by adsorption via π-complexation. Fluid Phase Equilib. **150**, 117–124 (1998a)

Blas, F.J., Vega, L.F., Gubbins, K.E.: Modeling new adsorbents for ethylene/ethane separations by adsorption via π-complexation. Fluid Phase Equilib. **150–151**, 117–124 (1998b)

Brandani, S., Hufton, J., Ruthven, D.: Self-diffusion of propane and propylene in 5A and 13X zeolite crystals studied by the tracer ZLC method. Zeolites **15**(7), 624–631 (1995)

Breck, D.W.: Zeolite Molecular Sieves. Wiley, New York (1974)

Cheng, L., Yang, R.: Monolayer cuprous chloride dispersed on pillared clays for olefin-paraffin separations by π-complexation. Adsorption **1**(1), 61–75 (1995)

Chmelik, C., Freude, D., Bux, H., Haase, J.: Ethene/ethane mixture diffusion in the MOF sieve ZIF-8 studied by MAS PFG NMR diffusometry. Microporous Mesoporous Mater. **147**(1), 135–141 (2012)

Choi, B.-U., Choi, D.-K., Lee, Y.-W., Lee, B.-K., Kim, S.-H.: Adsorption equilibria of methane, ethane, ethylene, nitrogen, and hydrogen onto activated carbon. J. Chem. Eng. Data **48**(3), 603–607 (2003)

Choudary, N.V., Kumar, P., Bhat, T.S.G., Cho, S.H., Han, S.S., Kim, J.N.: Adsorption of light hydrocarbon gases on alkene-selective adsorbent. Ind. Eng. Chem. Res. **41**(11), 2728–2734 (2002)

Chudasama, C.D., Sebastian, J., Jasra, R.V.: Pore-size engineering of zeolite A for the size/shape selective molecular separation. Ind. Eng. Chem. Res. **44**(6), 1780–1786 (2005)

Costa, E., Calleja, G., Marron, C., Jimenez, A., Pau, J.: Equilibrium adsorption of methane, ethane, ethylene, and propylene and their mixtures on activated carbon. J. Chem. Eng. Data **34**(2), 156–160 (1989)

Da Silva, F.A., Rodrigues, A.E.: Adsorption equilibria and kinetics for propylene and propane over 13X and 4A zeolite pellets. Ind. Eng. Chem. Res. **38**(5), 2051–2057 (1999)

Da Silva, F.A., Rodrigues, A.E.: Vacuum swing adsorption for propylene/propane separation with 4A zeolite. Ind. Eng. Chem. Res. **40**(24), 5758–5774 (2001)

Dewitt, A.C., Herwig, K.W., Lombardo, S.: Adsorption and diffusion behavior of ethane and ethylene in sol-gel derived microporous silica. Adsorption **11**(5–6), 491–499 (2005)

Do, D.: Adsorption Analysis: Equilibria and Kinetics. Series on Chemical Engineering, vol. 2. Imperial College Press, London (1998)

Eldridge, R.B.: Olefin/paraffin separation technology: a review. Ind. Eng. Chem. Res. **32**(10), 2208–2212 (1993)

Fuertes, A.B., Menendez, I.: Separation of hydrocarbon gas mixtures using phenolic resin-based carbon membranes. Sep. Purif. Technol. **28**(1), 29–41 (2002)

Giannakopoulos, I.G., Nikolakis, V.: Separation of propylene/propane mixtures using faujasite-type zeolite membranes. Ind. Eng. Chem. Res. **44**(1), 226–230 (2004)

Gilliland, E.R., Bliss, H.L., Kip, C.E.: Reaction of olefins with solid cuprous halides. J. Am. Chem. Soc. **63**(8), 2088–2090 (1941)

Gilliland, E.R., Seebold, J.E., FitzHugh, J.R., Morgan, P.S.: Reaction of olefins with solid cuprous halides. J. Am. Chem. Soc. **61**(8), 1960–1962 (1939)

Grande, C.A., Araujo, J.D.P., Cavenati, S., Firpo, N., BASALDELLA, E., Rodrigues, A.E.: New π-complexation adsorbents for propane–propylene separation. Langmuir **20**(13), 5291–5297 (2004)

Grande, C.A., Cavenati, S., Barcia, P., Hammer, J., Fritz, H.G., Rodrigues, A.E.: Adsorption of propane and propylene in zeolite 4A honeycomb monolith. Chem. Eng. Sci. **61**(10), 3053–3067 (2006)

Grande, C.A., Gascon, J., Kapteijn, F., Rodrigues, A.E.: Propane/propylene separation with Li-exchanged zeolite 13X. Chem. Eng. J. **160**(1), 207–214 (2010)

Grande, C.A., Gigola, C., Rodrigues, A.E.: Adsorption of propane and propylene in pellets and crystals of 5A zeolite. Ind. Eng. Chem. Res. **41**(1), 85–92 (2001)

Grande, C.A., Rodrigues, A.E.: Adsorption of binary mixtures of propane–propylene in carbon molecular sieve 4A. Ind. Eng. Chem. Res. **43**(25), 8057–8065 (2004)

Grande, C.A., Rodrigues, A.E.: Propane/propylene separation by pressure swing adsorption using zeolite 4A. Ind. Eng. Chem. Res. **44**(23), 8815–8829 (2005)

Hirai, H., Hara, S., Komiyama, M.: Polystyrene-supported aluminium silver chloride as selective ethylene adsorbent. Die Angewandte Makromolekulare Chemie **130**(1), 207–212 (1985a)

Hirai, H., Kurima, K., Wada, K., Komiyama, M.: Selective ethylene adsorbents composed of copper(I) chloride and polystyrene resins having amino groups. Chem. Lett. **14**(10), 1513–1516 (1985b)

Iucolano, F., Aprea, P., Caputo, D., Colella, C., Eić, M., Huang, Q.: Adsorption and diffusion of propane and propylene in Ag+-impregnated MCM-41. Adsorption **14**(2–3), 241–246 (2008)

Jiang, D.-E., Sumpter, B.G., Dai, S.: Olefin adsorption on silica-supported silver salts—a DFT study. Langmuir **22**(13), 5716–5722 (2006)

Kuznicki S. M., US Patent 4,938,939, 1990

Lee, Y., Reisner, B.A., Hanson, J.C., Jones, G.A., Parise, J.B., Corbin, D.R., Toby, B.H., Freitag, A., Larese, J.Z.: New insight into cation relocations within the pores of zeolite rho: in situ synchrotron X-ray and neutron powder diffraction studies of Pb- and Cd-exchanged rho. J. Phys. Chem. B **105**(30), 7188–7199 (2001)

Myers, A.L., Prausnitz, J.M.: Thermodynamics of mixed-gas adsorption. AIChE J. **11**, 121–127 (1965)

Li, K., Olson, D.H., Seidel, J., Emge, T.J., Gong, H., Zeng, H., Li, J.: Zeolitic imidazolate frameworks for kinetic separation of propane and propene. J. Am. Chem. Soc. **131**(30), 10368–10369 (2009)

Lin, C.C.H., Sawada, J.A., Wu, L., Haastrup, T., Kuznicki, S.M.: Anion-controlled pore size of titanium silicate molecular sieves. J. Am. Chem. Soc. **131**(2), 609–614 (2008)

Mathias, P.M., Kumar, R., Moyer, J.D., Schork, J.M., Srinivasan, S.R., Auvil, S.R., Talu, O.: Correlation of multicomponent gas adsorption by the dual-site langmuir model. Application to nitrogen/oxygen adsorption on 5A-zeolite. Ind. Eng. Chem. Res. **35**(7), 2477–2483 (1996)

Murthi, M., Snurr, R.Q.: Effects of molecular siting and adsorbent heterogeneity on the ideality of adsorption equilibria. Langmuir **20**(6), 2489–2497 (2004)

Nakahara, T., Wakai, T.: Adsorption of ethylene/ethane mixtures on a carbon molecular sieve. J. Chem. Eng. Data **32**(1), 114–117 (1987)

Olivier, M.-G., Bougard, J., Jadot, R.: Adsorption of propane, propylene and propadiene on activated carbon. Appl. Therm. Eng. **16**(5), 383–387 (1996)

Padin, J., Rege, S.U., Yang, R.T., Cheng, L.S.: Molecular sieve sorbents for kinetic separation of propane/propylene. Chem. Eng. Sci. **55**(20), 4525–4535 (2000)

Padin, J., Yang, R.T.: New sorbents for olefin/paraffin separations by adsorption via π-complexation: synthesis and effects of substrates. Chem. Eng. Sci. **55**(14), 2607–2616 (2000)

Park, J.-H., Han, S.-S., Kim, J.-N., Cho, S.-H.: Vacuum swing adsorption process for the separation of ethylene/ethane with $AgNO_3$/clay adsorbent. Korean J. Chem. Eng. **21**(1), 236–245 (2004)

Rege, S.U., Padin, J., Yang, R.T.: Olefin/paraffin separations by adsorption: π-complexation vs. kinetic separation. AIChE J. **44**(4), 799–809 (1998)

Romero-Pérez, A., Aguilar-Armenta, G.: Adsorption kinetics and equilibria of carbon dioxide, ethylene, and ethane on 4A(CECA) zeolite. J. Chem. Eng. Data **55**(9), 3625–3630 (2010)

Ruthven, D.: Gas separation by adsorption processes by Ralph T. Yang, Butterworths, Boston 1986. Can J Chem Eng **67**(1), 174 (1989)

Silva, F.A.D., Rodrigues, A.E.: Propylene/propane separation by vacuum swing adsorption using 13X zeolite. AIChE J. **47**(2), 341–357 (2001)

Sircar, S., and A. L. Myers. 2003. Gas separation by zeolites

Sá Gomes, P., Lamia, N., Rodrigues, A.E.: Design of a gas phase simulated moving bed for propane/propylene separation. Chem. Eng. Sci. **64**(6), 1336–1357 (2009)

Tang, Z., Dong, J., Nenoff, T.M.: Internal surface modification of MFI-type zeolite membranes for high selectivity and high flux for hydrogen. Langmuir **25**(9), 4848–4852 (2009)

Timofeev, D.P., Erashko, I.T.: Sorption kinetics of water vapor on type a zeolites. Bull Acad Sci USSR, Div Chem Sci **10**(7), 1105–1109 (1961)

Van Miltenburg, A., Zhu, W., Kapteijn, F., Moulijn, J.A.: Adsorptive separation of light olefin/paraffin mixtures. Chem. Eng. Res. Des. **84**(5), 350–354 (2006)

Wang, S., Yang, Q., Zhong, C.: Adsorption and separation of binary mixtures in a metal-organic framework Cu-BTC: a computational study. Sep. Purif. Technol. **60**(1), 30–35 (2008)

Wu, Z., Han, S.-S., Cho, S.-H., Kim, J.-N., Chue, K.-T., Yang, R.T.: Modification of resin-type adsorbents for ethane/ethylene separation. Ind. Eng. Chem. Res. **36**(7), 2749–2756 (1997)

Yang, R. T. 1986. Gas separation by adsorption processes

Yang, R.T., Kikkinides, E.S.: New sorbents for olefin/paraffin separations by adsorption via π-complexation. AIChE J. **41**(3), 509–517 (1995)

Yoon, J.W., Jang, I.T., Lee, K.Y., Hwang, Y.K., Chang, J.-S.: Adsorptive separation of propylene and propane on a porous metal-organic framework, copper trimesate. Bull. Korean Chem. Soc. **31**(1), 220–223 (2010)